1ST INTERNATIONAL CONFERENCE ON PHONONIC CRYSTALS, METAMATERIALS & OPTOMECHANICS

Extended Abstracts

Track 6: Fabrication and Characterization for Phononics

Phononics 2011: First International Conference on Phononic Crystals, Metamaterials and Optomechanics
Santa Fe, New Mexico, USA, May 29-June 2, 2011
PHONONICS-2011-0038

Nanoscale Tip Fabrication for Plasmon Induced Field-Enhancement

Won S. Chang[1] , Sung-H. Cho[1]

[1] *Nano Convergence and Manufacturing Systems Research Division, KIMM, 171 Jang-dong Yuseong-gu Daejeon, 305-343, South Korea,*
paul@kimm.re.kr, shcho@kimm.re.kr

Abstract: Nanoscale tip is designed for enhancement of optical resolution of near-field scanning optical microscopy (NSOM). To fabricate a tip-on-aperture NSOM probe, a tip is generated at the end of the probe. Focused ion beam (FIB) process is applied to the process to make an aperture and a tip, so the aperture and the tip are generated at the same time. With this process, possibilities tofabricate tip-on-aperture probes with various tips were shown.

The resolution of commercial optical system is limited to about the wavelength of incident light by the refraction limit. However, a resolution beyond the diffraction limit can be achieved at near-field. Near-field scanning optical microscope (NSOM) is a kind of scanning probe microscope; it can realize a sub-wavelength scale resolution. In NSOM, light is illuminated through an aperture smaller than the wavelength of incident light, and then the small aperture is used as an excitation source. The resolution of the NSOM is determined by the size of the aperture; to achieve a higher resolution, a smaller aperture is required. However, when the diameter of an aperture is smaller than the wavelength of the incident light, the transmission efficiency is proportional to the sixth power of the diameter of the aperture. Thus, a smaller aperture greatly reduces the transmission efficiency. To obtain a sufficiently strong signal from a small aperture, high-intensity light is needed[1]. However, high-intensity light can damage the metal layer of the probe. The typical resolution of aperture NSOM is about 50 nm – 100 nm. In this work, the shape of a NSOM probe was modified using the resolution of numerical analysis based on a finite-difference time-domain (FDTD) algorithm. This probe has a narrow slit or small tip on its aperture. Especially in the near-field area, the electric field intensity distribution is heavily dependent on the polarization of incident light. In the plane of polarization, the electric field intensity of the NSOM aperture probe is strongly enhanced at the edge of the aperture. Simulation results show that this enhancement can be totally or partially removed according to the size of the slit, if the slit carved on the probe is aligned with the polarization direction of the incident light. When a long slit is carved on the probe (slit-on-aperture probe), the electric field intensity of the NSOM aperture probe in the plane of polarization shows a Gaussian distribution because the points of enhanced electric field intensity are totally removed. However, when a short slit is carved on the probe, the point of enhanced electric field intensity is removed at one edge of the aperture, and consequently the electric field intensity is enhanced only at the other edge. Moreover, when a tip is put on the probe (tip-on-aperture probe), the electric field intensity is enhanced only near the tip. This means that a higher intensity electric field can be obtained on the surface to be processed in an area smaller than the aperture size.
The tip of a tip-on-aperture (TOA) probe is illuminated through an aperture at the near-field of the probe and electromagnetic interaction between the structure sharp tip at the end of the probe and the surface is used for measurements and materials processing. A novel TOA probe is described, which has a polygonal cross-sectioned tip that can make the strong and local enhancement of electromagnetic field[3,4]. A right triangular pillar was selected as optimal shape of the tip among the several polygonal pillars. The electromagnetic energy distributions at the near-field of the probe and of a typical TOA probe (with circular tip) were calculated numerically, and the results were analyzed. The results show that a TOA probe with a triangle tip confines electromagnetic energy within the smaller area than a typical tip-on-aperture probe, and has 6.7 times the maximum intensity. Moreover, the electric field distributions at the near-field of a TOA probe were calculated numerically to analyze the effects of polarization direction on the characteristics of measurement and processing. A TOA probe is asymmetric for the axis, since it has a probe at metal coated layer on the aperture. The geometrical relationship between this asymmetric shape and polarization direction is the reason for the change of the electromagnetic energy distributions. Numerical analysis shows that a TOA probe can make the best use of the tip for high resolutions when the tip is located on the parallel axis with the polarization

Phononics 2011: First International Conference on Phononic Crystals, Metamaterials and Optomechanics
Santa Fe, New Mexico, USA, May 29-June 2, 2011
PHONONICS-2011-0038

direction. After analyzing the trend in the magnitude of the electric field, it was proposed that a localized, enhanced field at the tip apex was caused by the local electric field at the aperture and surface plasmons excited and propagating on the outer surface of the probe.
An NSOM probe is a tinned, metal coated optical fiber with an aperture. To fabricate a TOA NSOM probe, a tip is generated at the end of the probe. FIB processing is applied to the process to make an aperture and a tip, so the aperture and the tip are generated at the same time. With this process, possibilities to fabricate TOA probes with various tips and were shown. And resolution enhancement for optical measurement and patterning was verified using the TOA probe fabricated in this study.

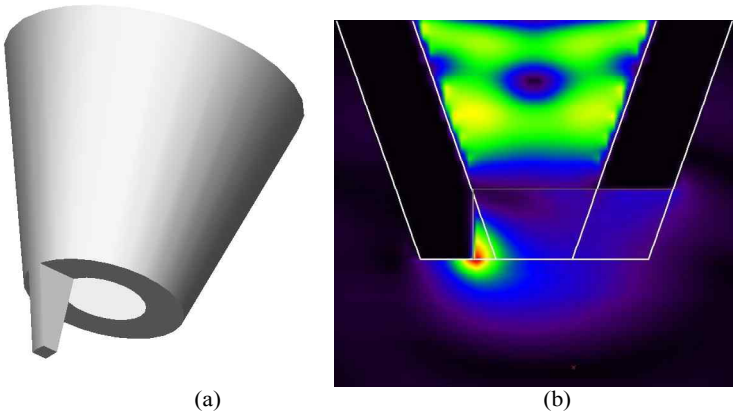

(a) (b)

Figure 1 (a) Three-dimensional modeling of nanoscale tip on NSOM probe and (b) FDTD analysis of electric field distribution on TOA probe

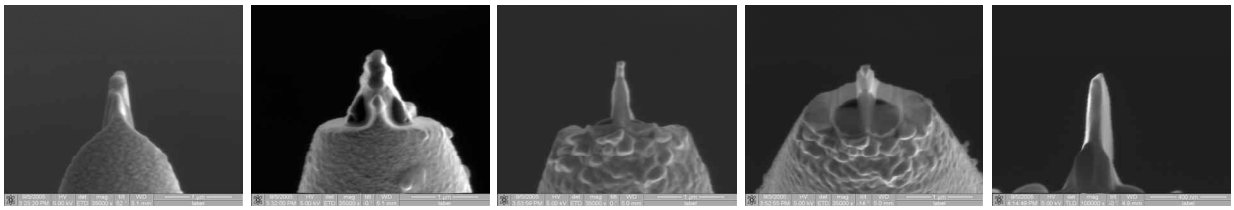

Figure 2 FIB machined TOA probe on fiber NSOM probe

References

[1] M. Stähelin, M. A. Bopp, G.. Tarrach, A. J. Meixner, and I. Zschokke-Gränacher: *Appl. Phys. Lett*. **68** 2603 (1996).
[2] T. Matsumoto, T. Ichimura, T. Yatsui, M. Kourohi, T. Saiki, and M. Ohtsu: *Opt. Rev*. **5** 369 (1998).
[3] H. G. Frey, F. Keilmann, A. Kriele, and R. Guckenberger: *Appl. Phys. Lett.* **81** 5030 (2002).

Phononics 2011: First International Conference on Phononic Crystals, Metamaterials and Optomechanics
Santa Fe, New Mexico, USA, May 29-June 2, 2011
PHONONICS-2011-0075

Larger Scale Fabrication of Nanometer to Micron Sized Periodic Structures in 2D and 3D: Approaches and Trends

Gregory R. Bogart[1]

[1] *Sandia National Laboratories, P.O. Box 5800 MS1080, Albuquerque, NM, USA*
grbogar@sandia.gov

Fabrication of periodic structures for photonic or phononic wavelength interaction and manipulation at the small scale (<100um x 100 um) in planar dimensions using a variety of materials and techniques has been documented in the literature. Often structures are conceived and built with only a single device needing to be made. Some applications require that structures be fabricated in three dimensions or with multiple layers placing additional constraints on the fabricator. If a structure proves to be useful and a demand to have it appears, the researcher is often asked, "Can you make more of it?" The challenge to manufacture larger, better structures, and more of them is not new in the history of product innovation and manufacture. However, the combination of requirements for accurate microscopic dimensional control over large spatial scale needed to make useful devices requires both out of the box thinking to manufacture them and familiarity and the ability to adapt tried and true scaling techniques.

Human ingenuity and desire for efficiency has used the "stamp" for thousands of years to impart a repeated pattern into materials that served, speed, ease of use, and functionality requirements. Signet rings or "seals" were used with waxes or inks to authenticate the earliest hand written documents and are still in use today. (1) The method of placing multiple patterns or individual stamps next to each other surfaced in China in the early 11th century (2). Combining the patterns with a proper substrate material (paper) made communication easier and faster. Researchers in photonic crystal fabrication have leveraged the established stamping technique to deliver fabrication of large area 3D photonic crystal designs. Instead of clay tablets, engineered siloxanes have allowed for durable and re-usable stamps that are able to replicate the molded features at the nanometer scale. The stamping technique can be enhanced by combining with well established optical principles to generate three dimensional periodic structures. Further leveraging sophisticated modeling, semiconductor processes and engineered materials enables fabrication of large area, three dimensional periodic structures with submicron features. Figure 1a is a photograph of a large area silicone based stamp used to imprint phase masks into the surface of photo resists. Figure 1b is a photograph showing the diffraction pattern created by the phase mask using collimated light (3).

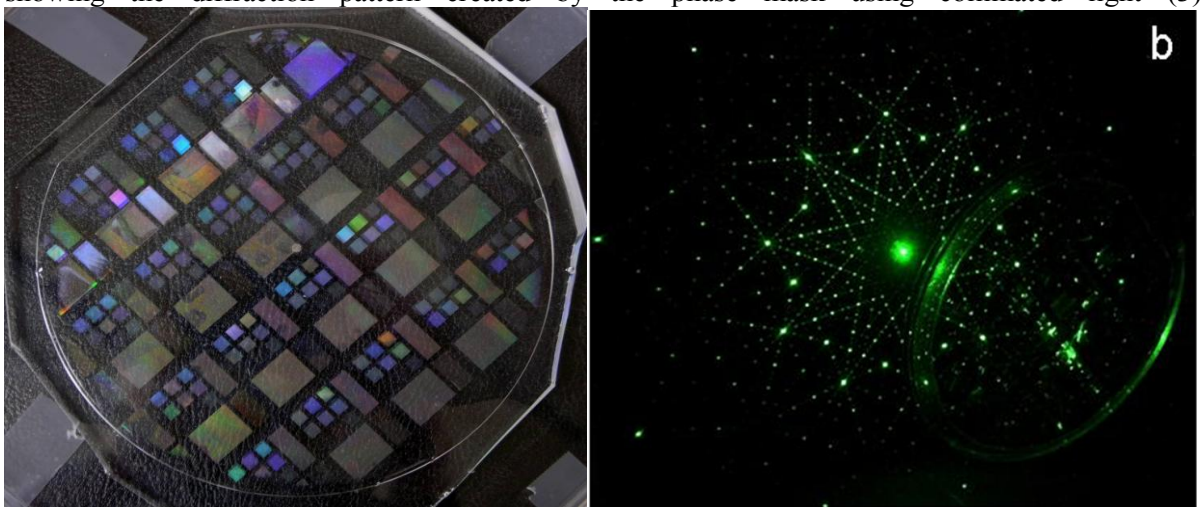

Figure 1. a.) 150mm diameter stamp master for proximity nano patterning of quasi crystal pattern. b.) diffraction pattern generated using an engineered phase mask.

Phononics 2011: First International Conference on Phononic Crystals, Metamaterials and Optomechanics
Santa Fe, New Mexico, USA, May 29-June 2, 2011
PHONONICS-2011-0075

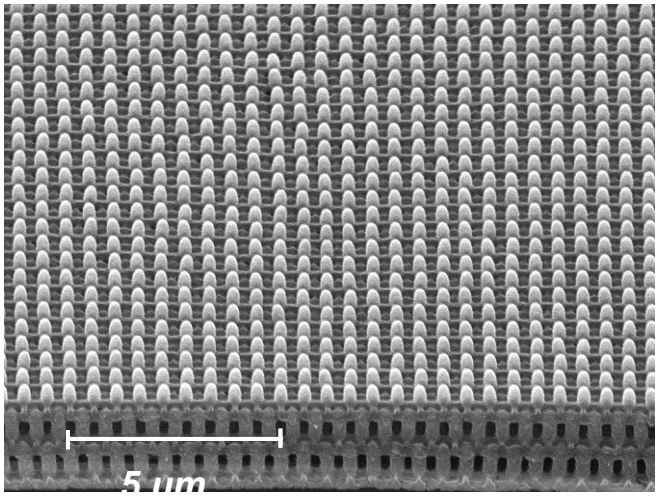

Figure 2. Cross section SEM of a resist structure generated with a stamped phase mask on the surface of the resist.

Collimated light used for exposure combined with the surface relief generated by the stamp creates constructive and destructive interference patterns in three dimensions. Figure 2 contains a cross sectional scanning electron micrograph of exposed and developed photoresist using an optical phase mask generated with a stamped surface and optical interference. Note the periodic nature in all three dimensions.

Many materials that are suitable for optoelectronics and CMOS device manufacturing are also finding uses in the phononics area. Lithium niobate has been used extensively in optoelectronic fabrication due to its desirable optical properties. It is particularly challenging to process using conventional CMOS process techniques as it is both pyroelectric and piezoelectric. Processing limitations can impact the usefulness and implementation of these materials.

Large scale fabrication of these types nanometer sized periodic structures requires an integrated approach. In this presentation I will review other scaling approaches to making large area phononic or photonic crystals in 2D and 3D such as direct write and self assembly. In addition, I will touch on the necessary infrastructure required to develop these techniques including modeling, design, and material considerations appropriate for the various methods. Lastly, I will discuss future trends of the technology.

References: 1.) Kipfer, B. A. , Encylcopedic Dictionary of Archaeology. Springer, 2000 (501)

2.) Day, L., McNeil I.; Biographical Dictionary of the History of Technology. Taylor and Francis, 1998 (123)

3.) Shir, D.J, et al. ; Tharee-Dimensiional Nanofabrication with Elastomeric Phase Masks, Journal of Physical Chemistry B 111, 12945-12958 (2007)

Sandia is a multiprogram laboratory operated by Sandia Corporation, a Lockheed Martin Company, for the United States Department of Energy under contract DE-AC04-94AL85000.

Phononics 2011: First International Conference on Phononic Crystals, Metamaterials and Optomechanics
Santa Fe, New Mexico, USA, May 29-June 2, 2011
PHONONICS-2011-0105

Microfabricated GHz Phononic Band Gap Structures

Gianluca Piazza, Nai-Kuei Kuo

Department of Electrical and Systems Engineering, University of Pennsylvania, Philadelphia, PA, 19104, USA
piazza@seas.upenn.edu, kuo1@seas.upenn.edu

Abstract: This paper reports the latest development on the synthesis of phononic band gaps (PBG) in AlN/Air and SiC/Air structures operating in the GHz range by means of inverted cylindrical geometries or fractal-based designs. Finite element methods used to design and confirm the PBG dispersion curve and amplitude-frequency response are also presented.

Microscale phononic crystals (PC) have emerged as a new class of devices that can be employed to understand and engineer the fundamental properties of low loss acoustic materials at the nanoscale, demonstrate novel acoustic functionalities such as tunneling, waveguiding and multiplexing and synthesize miniaturized and low loss radio frequency (RF) signal processors that are not attainable with state-of-the-art micro/nano mechanical (M/NEMS) resonators. Since the introduction of PCs in 1998, PC-based devices such as wave guides, filters and structures for acoustic focusing have been demonstrated, but are all limited in operating frequencies below 1 MHz due to their fabrication by means of hand-assembly. Recently, via microfabrication techniques, substantial progress has been made in extending PC structures in the very and ultra high frequency (VHF and UHF) range [1-3]. The extension of the frequency range of these PC-based devices makes them amenable to applications in RF communications.

Within PCs, Phononic Band Gaps (PBG) are the most important building blocks. PBG structures form frequency ranges in which the propagation of specific elastic waves is prohibited by the size, periodicity and arrangement of a unit cell. Most of the micromachined PC demonstrations to date have been either limited to low MHz frequencies when using air/solid configurations, or have used complex manufacturing processes relying on several refill and planarization steps when pushed close to 1 GHz.

To synthesize PBGs that can be easily microfabricated and integrated with electro-acoustic transducers, we have designed and experimentally demonstrated new classes of PCs that rely on alternating in two dimensions (2D) regions of high acoustic velocity and low loss materials such as aluminum nitride, or silicon carbide with air (low acoustic velocity material) (Fig. 1-3). Unit cell geometries in the form of a cylinder supported by four tethers (inverted configuration with respect to the conventional cylindrical air hole) (Fig. 1), an X-shape (Fig. 2) or a fractal-based square design (Fig. 3) have been introduced to reduce the manufacturing constraints associated with either the film thickness or the lithographically defined in-plane dimensions, so that operation between 500 MHz and 1 GHz could be attained. The selection of AlN or SiC as the structural layer for the definition of the PBG unit cell was made to gain access to some of the highest acoustic velocity materials with low losses that are easily integrated with electro-acoustic AlN transducers.

The experimental results (Fig. 1-3) confirm the existence of the designed PBGs, show high rejection and match the theoretical analysis performed via COMSOL Finite Element Methods (FEM). Frequency dispersion response curves predicting the presence of full or longitudinal-wave-specific band gaps (Fig. 1-3) were obtained by 3D eigenfrequency analysis of the unit cell block on which periodic boundary conditions had been applied according to the Bloch theorem. Amplitude-frequency response curves (Fig. 2) that reproduce the experimentally-obtained transmission data were simulated in COMSOL FEM by performing a frequency sweep in the acoustic module and using perfectly matched layers at the edges of the PBG in order to accurately model acoustic adsorption. A single row of unit cells was modeled and periodic conditions in the 3rd direction were assumed.

The reported experimental and modeling efforts lay the foundations for the synthesis of GHz PC devices that will find practical applications in RF communication systems.

References

1. Olsson, R.H., III and I. El-Kady, *"Microfabricated phononic crystal devices and applications"*, Measurement Science & Technology, 2009, **20**(1), p. 012002 (13 pp.).
2. Mohammadi, S., et al., *"Evidence of large high frequency complete phononic band gaps in silicon phononic crystal plates"*, Applied Physics Letters, 2008, **92**(22), p. 221905-1.

Phononics 2011: First International Conference on Phononic Crystals, Metamaterials and Optomechanics
Santa Fe, New Mexico, USA, May 29-June 2, 2011
PHONONICS-2011-0105

3. Xinya, Z., et al., "*Evidence of surface acoustic wave band gaps in the phononic crystals created on thin plates",* Applied Physics Letters, 2006, **88**(4), p. 41911-1.

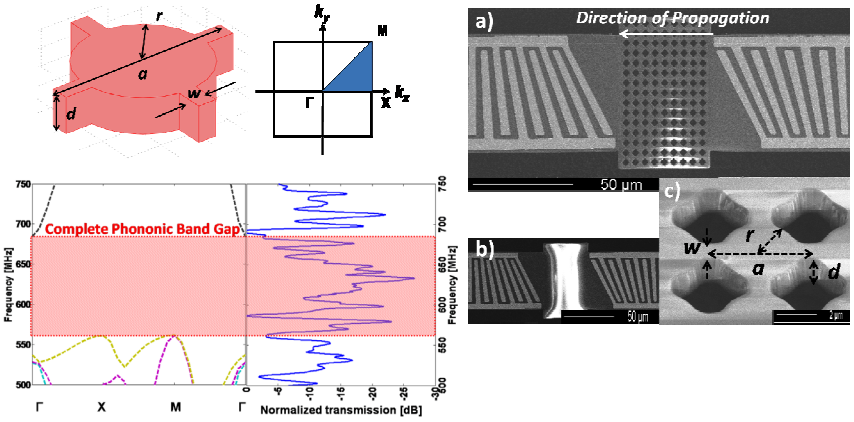

Figure 1: AlN/Air inverted cylinder PBG: (top-left) unit cell geometry and first symmetric Bruillon zone for square lattice; (right) SEM of PBG integrated with AlN electro-acoustic transducers; (bottom-left) dispersion curve and amplitude-frequency experimental response of this PBG.

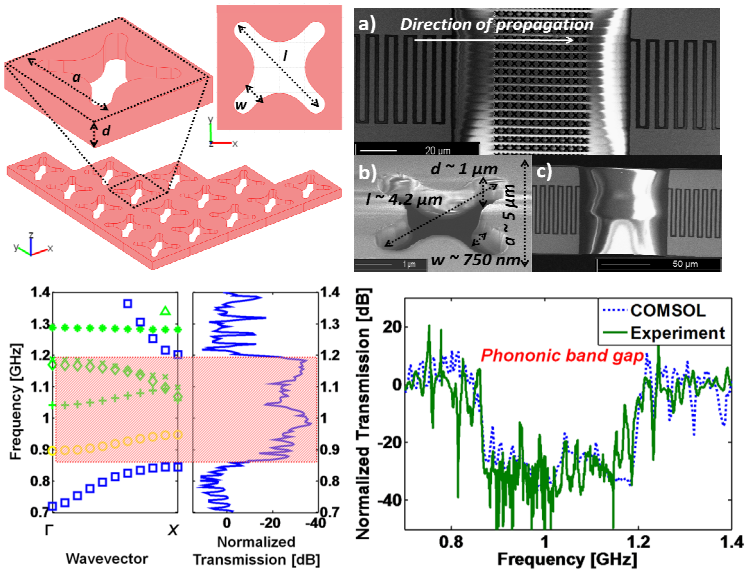

Figure 2: AlN/Air X-shaped PBG: (top-left) unit cell geometry and periodic arrangement; (top-right) SEM of PBG integrated with AlN electro-acoustic transducers; (bottom-left) dispersion curve and amplitude-frequency response obtained by COMSOL FEM for this PBG; (bottom-right) normalized experimental transmission response compared to COMSOL FEM analysis.

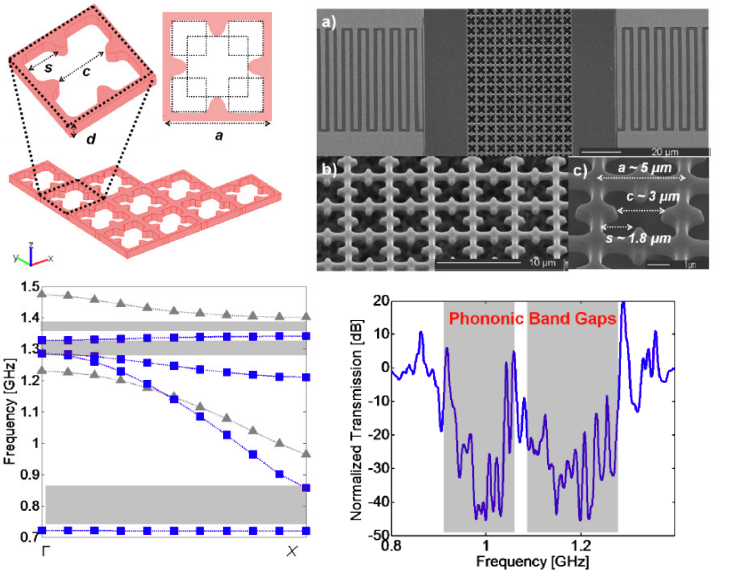

Figure 3: SiC/Air fractal-based PBG: (top-left) unit cell geometry and periodic arrangement; (top-right) SEM of PBG integrated with AlN electro-acoustic transducers; (bottom-left) dispersion curve obtained by COMSOL FEM for this PBG; (bottom-right) normalized experimental transmission response.

Phononics 2011: First International Conference on Phononic Crystals, Metamaterials and Optomechanics
Santa Fe, New Mexico, USA, May 29-June 2, 2011
PHONONICS-2011-0113

Thermal Conductivity Reduction in Lithographically Patterned Single Crystal Silicon Phononic Crystal Structures

Bongsang Kim[1], Janet Nguyen[1,2], Eric A Shaner[1], Ihab El-Kady[1], Roy H. Olsson III[1]

[1] *Department of Advanced MEMS, Sandia National Laboratories, NM, USA*
bonkim@sandia.gov, jhnguyen@sandia.gov, eashane@sandia.gov, ielkady@sandia.gov, rholsso@sandia.gov
[2] *Department of Electrical and Computer of Engineering, University of New Mexico, NM, USA*

Abstract: In-plane thermal conductivity of lithography-based phononic crystals has been investigated. Sub-micron holes were lithographically patterned in a 500nm-thick single crystal silicon thin-film and the thermal conductivity was measured as low as 30 W/mK (at and slightly above room temperature, 20~80°C), which is a 50% reduction even after accounting for the effect of volume reduction of the holes.

Thermal conductivities of many materials used in micro/nano-machining, such as silicon, have shown dramatic reduction in micro/nano-scale structures[1]. In such materials, the dominating heat transfer mechanism is through lattice vibration (phonons). Therefore, as the dimensions of thermal pathways become comparable to the phonon mean-free-path, phonon scattering increases, resulting in reduction in thermal conductivity. Recently, researchers have demonstrated successful control over thermal conductivity by patterning periodic nano-holes in a silicon membrane[2]. Despite such promising results, however, due to complexity of the fabrication processes and lack of effective integration methods, very few examples of application could be found among the demonstrated structures. Alternately, a much simpler way of phonon manipulation has been demonstrated with the recent advances in lithographic technologies. For example, phononic crystals were fabricated by lithographically defined sub-micron holes in a silicon layer to construct waveguides successfully achieving 30dB acoustic rejection at 67MHz for RF communication applications[3].

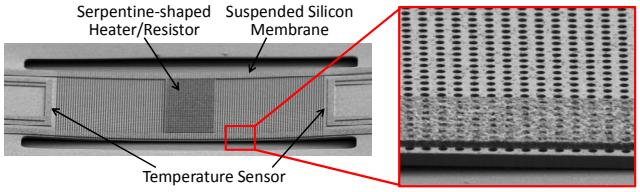

Figure 1 SEM image of a bridge-shaped test structure. Phononic crystals were formed by sub-micron diameter holes which were lithographically defined in a 500nm-thick single crystal silicon thin film.

In this work, we studied the effect of lithography-based phononic crystals on conductive heat transfer of single crystal silicon thin-film. Specifically, periodic sub-micron diameter through-holes were defined using a deep UV ASML scanner and patterned in a 500nm-thick silicon layer by plasma etching. To measure their in-plane thermal conductivity, a bridge-shaped test structure was designed as shown in Figure 1. A serpentine-shaped aluminum trace was placed in the middle and two temperature sensors were installed at the bridge edges. While heat is supplied to the aluminum trace at the center, the resistance change of each trace was measured to estimate the temperature increase. Temperature dependences of each trace resistance were separately calibrated by a heated chuck measurement. Figure 2 shows ANSYS finite element simulation and the equivalent thermal circuit model of the test structure. By using these models, the device thermal resistances and the thermal conductivity of the phononic crystal layers are calculated.

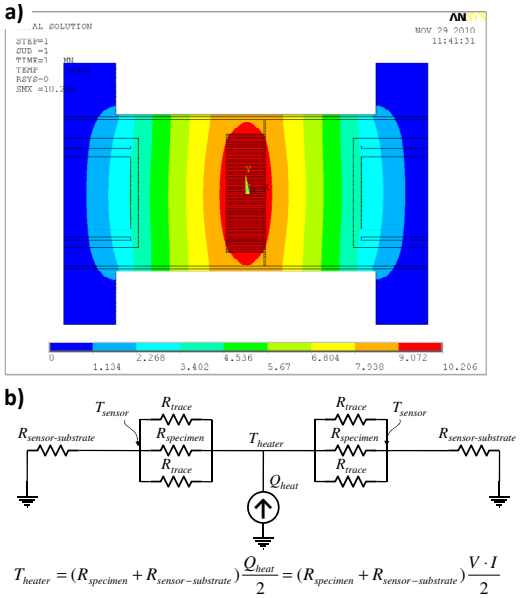

Figure 2 a) ANSYS finite element model and b) equivalent thermal circuit model of the test structure.

Phononics 2011: First International Conference on Phononic Crystals, Metamaterials and Optomechanics
Santa Fe, New Mexico, USA, May 29-June 2, 2011
PHONONICS-2011-0113

For each pitch-diameter combination a total of four samples were tested at and slightly above room temperature (20~80°C). The obtained thermal resistance, $R_{specimen}$, and thermal conductivity, $k_{measured}$, values from the measurement are summarized in Figure 3 and Table 1. The thermal conductivity of metric samples, which don't have any through holes, was measured as 97.8 W/mK, which is consistent with values from the literature[1]. In all measured samples, significant reductions in thermal conductivity could be observed. It is observed that the $k_{measured}$ values were much smaller than $k_{M\text{-}E}$, inferring the reduction in thermal conductivity is beyond the contribution from the volume reduction effect alone. ($k_{M\text{-}E}$ is the prediction of Maxwell-Eucken theory which models only the effect of volume reduction in porous materials[4].) The difference between the measured values and those predicted by the Maxwell-Eucken Model increases as the minimum feature size decreases, which is likely due to enhanced phonon scattering as the size of the thermal pathways shrink. Among tested samples, the device with 0.45um diameter holes with 0.70um pitch (limiting dimension is 0.25um) showed the highest reduction in thermal conductivity, i.e., $k_{measured}$ is 30W/mK which is only 30% of the metric sample's $k_{measured}$ and 50% of that predicted by the Maxwell-Eucken model, $k_{M\text{-}E.}$

This result indicates that material thermal conductivity can be effectively controlled via phonon-scattering enhancement from lithographically defined sub-micron features. The availability of such lithography-based phononic crystals has huge potential to open direct applications to many micromachined devices without much modification in the original fabrication process. For example, by reducing thermal conductivity with much less alteration in electrical conductivity, the use of lithographically patterned phonon manipulators will be able to significantly enhance the performance of micromachined thermoelectric coolers or energy harvesters.

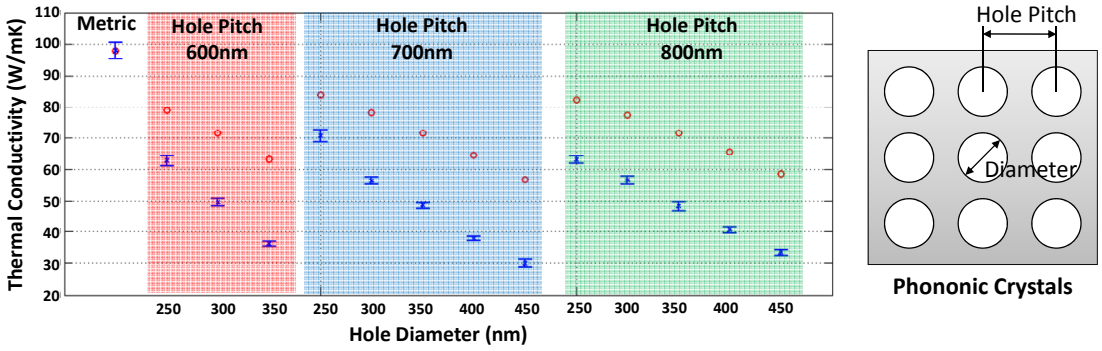

Figure 3 Measured thermal conductivities, $k_{measured}$ (blue error bars) and predicted thermal conductivities using Maxwell-Eucken Model, $k_{M\text{-}E}$ (red circles).

Pitch (nm)	1	0.6	0.6	0.6	0.7	0.7	0.7	0.7	0.7	0.8	0.8	0.8	0.8	0.8
Diameter (nm)	1	0.25	0.3	0.35	0.25	0.3	0.35	0.4	0.45	0.3	0.35	0.4	0.45	0.5
Porosity (%)	0	14	20	27	10	14	20	26	32	11	15	20	25	31
$R_{specimen}$ **(K/W)**	12247	18563	23046	30485	16640	20442	23490	29311	35862	18456	20408	23616	27519	32873
$k_{M\text{-}E}$ **(W/mK)**	97.8	79	71.5	63.2	83.8	78	71.5	64.4	56.8	82.4	77.3	71.5	65.4	58.8
$k_{measured}$ **(W/mK)**	97.8	62.7	49.5	36.2	70.6	56.5	48.5	37.8	30	63.1	56.6	48.2	40.6	33.2
$k_{measured}/k_{M\text{-}E}$ **(%)**	100	79	69	57	84	72	68	59	53	77	73	67	62	56

Table 1 Summary of measured thermal conductivities, $k_{measured}$, predicted thermal conductivities using Maxwell-Eucken Model, $k_{M\text{-}E}$, and their ratio for each sample.

References

[1] M. Asheghi, M. N. Touzelbaev, K. E. Goodson, Y. K. Leung, and S. S. Wong, *Journal of Heat Transfer* **120**, 30-36 (1998).
[2] J. Tang, H.-T. Wang, D. H. Lee, M. Fardy, Z. Huo, T. P. Russell, and P. Yang, *Nano Letters* **10**, 4279-4283 (2010).
[3] R. H. Olsson III, I. El-Kady, M. F. Su, M. R. Tuck, J. G. Fleming, *Sensors and Actuators A: Physical* **145-146**, 87-93 (2008).
[4] A. Eucken, *Forschung auf dem Gebiete des Ingenieurwesens*; VDIverlag g.m.b.h.: Dusseldorf, 1932, Ausgabe B, 3/4 VDI Forschungsheft 353.

Phononics 2011: First International Conference on Phononic Crystals, Metamaterials and Optomechanics
Santa Fe, New Mexico, USA, May 29-June 2, 2011
PHONONICS-2011-0122

Micromachined Phononic Band-Gap Crystals and Devices

Roy H. Olsson III[1], Bongsang Kim[1], Maryam Ziaei-Moayyed[1], Charles M. Reinke[1], Mehmet M. Su[2], Yasser M. Soliman[2], Zayd C. Leseman[2], Ihab El-Kady[1,2]

[1] Sandia National Laboratories, Albuquerque NM, USA
rholsso@sandia.gov, bonkim@sandia.gov, mziaeim@sandia.gov, cmreink@sandia.gov, ielkady@sandia.gov
[2] University of New Mexico, Albuquerque NM, USA
mfatihsu@ece.unm.edu, yasser.soliman@gmail.com, zleseman@unm.edu

Abstract: Micromachined phononic crystals are an emerging technology with applications in radio frequency communications, sensors and thermal energy harvesting. This paper presents work at Sandia National Laboratories in the realization of micromachined phononic crystal devices across a broad frequency range and in a number of material systems.

Phononic crystals are an emerging field poised to impact radio frequency (RF) communications[1], thermal management[2], acoustic imaging[1] and a number of other fields where phonon propagation and control leads to improved system performance. Over the past decade phononic crystals have been scaled from large hand assembled balls in acoustically lossy materials such as water and epoxy to micro and nano fabricated 2D structures realized in low loss materials operating at frequencies from 10 MHz to 10 GHz and beyond. Batch fabrication and the ability to co-integrate piezoelectric transducers with phononic crystals have lead to experimentation on a wide variety of geometries, materials and devices. The ability to suspend 2-D phononic crystals above the substrate using micromachining techniques has allowed for low loss phononic waveguides[1,3-4] and cavities[5-6] to be demonstrated. The wide range of materials available and the implications of finite membrane thickness require careful consideration when designing a phononic crystal for a specific application. Phononic crystals and devices have been studied theoretically and experimentally in numerous material systems including Si-air[2,4-5], SiC-air[6], AlN-air[7], Si-W[8] and SiO_2-W[3,9]. Phononic band gaps at GHz frequencies have been demonstrated in each of these material systems with complete phononic band-gap widths exceeding 10% of the center frequency and band gaps for longitudinal waves in excess of 50%. Solid-Solid phononic crystals based on tungsten inclusions in low impedance media have demonstrated less sensitivity to membrane thickness and lithography when compared to solid-air phononic crystals[10]. Certain devices, such as cavities, requiring very low material damping have been best realized in solid-air material systems using high-Q materials such as SiC. Recent results indicate that phononic crystals formed using both solid and air inclusions results in superior band-gap properties when compared to solid or air inclusions alone[9]. While much recent progress has been achieved in realizing micro and nano scale phononic crystals several challenges and opportunities are emerging including: the need for much wider bandwidth piezoelectric transducers for interrogating the phononic crystals, the ability to combine phononic and photonic crystals to increase phonon-photon interactions and for processing light signals in the acoustic regime and the introduction of non-linearity with phononic band-gap materials.

References

[1] R. H. Olsson III, and I. El-Kady, *Meas. Sci. Technol*. 20, 012002 (2009).
[2] P. E. Hopkins, C. M. Reinke, M. F. Su, R. H. Olsson, III, E. A. Shaner, Z. C. Leseman, J. R. Serrano, L. M. Phinney, and I. El-Kady, *Nano Lett.,* 11, (2011).
[3] R. H. Olsson-III, S. X. Griego, I. El-Kady, M. F. Su, Y. M. Soliman, D. F. Goettler, and Z. C. Leseman, IEEE Ultrasonics Symp., 1150-1153 (2009).
[4] S. Mohammadi, A. A. Eftekhar, W. D. Hunt, A. Adibi, IEEE Freq. Cntrl. Symp., 768-772 (2008).
[5] M. Ziaei-Moayyed, M. F. Su, C. M. Reinke, I. El-Kady, and R. H. Olsson III, IEEE Ultrasonics Symp., (2010).
[6] S. Mohammadi, A. A. Eftekhar, A. Khelif, H. Moubchir, W. D. Hunt, and A. Adibi, *Appl. Phys. Lett.*, **95**, 051906 (2009).
[7] N. Kuo, C. Zuo, and G. Piazza, *Appl. Phys. Lett.* **95**, 093501 (2009).
[8] Y. M. Soliman, M. F. Su, Z. C. Leseman, C. M. Reinke, I. El-Kady, and R. H. Olsson III, *Appl. Phys. Lett.* **97**, 193502 (2010).
[9] M. F. Su, R. H. Olsson III, Z. C. Leseman, and I. El-Kady, *Appl. Phys. Lett.* **96**, 053111 (2010).
[10] C. M. Reinke, M. F. Su, R. H. Olsson III, and I. El-Kady, *Appl. Phys. Lett.,* In-Press (2011).

Phononics 2011: First International Conference on Phononic Crystals, Metamaterials and Optomechanics
Santa Fe, New Mexico, USA, May 29-June 2, 2011
PHONONICS-2011-0122

Phononics 2011: First International Conference on Phononic Crystals, Metamaterials and Optomechanics
Santa Fe, New Mexico, USA, May 29-June 2, 2011
PHONONICS-2011-0125

Fabrication of 2-D Phononic Crystals via Focused Ion Beam

D. F. Goettler[1], M. F. Su[1], R. H. Olsson III[2], I. El-Kady[2], and Z. C. Leseman[1]

[1] *Mechanical Engineering, University of New Mexico, Albuquerque, NM USA 87131*
goettled@unm.edu, mfatihsu@unm.edu, and zleseman@unm.edu
[2] *Sandia National Laboratories, Albuquerque, NM USA 87105*
rholsso@sandia.gov and ielkady@sandia.gov

Abstract: A technique for the fabrication of 2-D Phononic Crystals (PnCs) is described that utilizes a focused ion beam (FIB) instrument. In particular, the details of the microfabrication procedure are discussed which creates the main structure from which the PnC is created. Following the microfabrication is the nanoFIBrication of the microstructure to create a PnC with nanoscale features. Results will be presented for the fabrication of a 33 GHz PnC.

In order to achieve PnCs that operate above 10 GHz nanofabrication techniques will need to be utlized. PnCs that manipulate phonons above even 1 GHz have shown a tremendous ability to alter the thermal conductivity of materials[1]. In order to achieve an operating frequency above 10 GHz the dimensions of the inclusions on the lattice points and their spacing need to be < 100 nm. We have recently utilized a FIB instrument to attain PnCs with these dimensions.

The following is a discussion on the method we have recently utilized to create a PnC that has a bandgap at 33 GHz. Fabrication is a two part process. First, the microstructure from which the PnC is created is fabricated by standard microfabrication procedures. Then the nanostructure of the PnC can be defined using the FIB via nanoFIBrication.

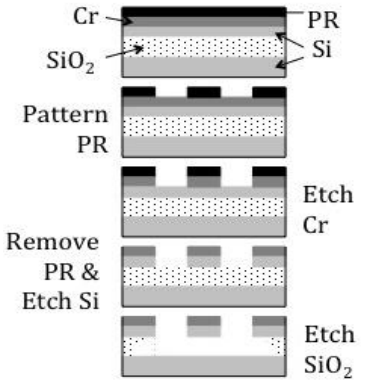

Figure 1: Fabrication process for creating a thin, freestanding membrane for 2-D PnC's

The scaffolding of the PnC is initially microfabricated using a silicon-on-insulator (SOI) wafer. Our group's studies show that thin membranes produce a bandgap that is unaltered by slab modes[2]. In particular, the thickness of the membrane from which the 2-D PnC is to be made must be less than the lattice spacing. The SOI is initially thinned down using alternating oxidations and HF etches. A protective layer of Cr is evaporated onto the SOI's device layer and then patterned. The BOX layer is then etched leaving a freestanding Si membrane on which the 2-D PnC will be defined. The full process is illustrated in Figure 1.

Using a FIB instrument we have been successful in creating a 33 GHz phononic crystal on the Si membrane. The PnC is composed of a Si matrix (the membrane) with W inclusions placed in a square array. The Si matrix was a freestanding membrane that was 100 nm thick and 10 x 10 μm area. Holes 30 nm in diameter were milled with the ion beam and subsequently backfilled with W using an e-beam deposition method.

Figure 2 shows details of the fabricated PnC. The leftmost image shows a 10 μm x 10 μm freely suspended membrane tethered on either side to the SOI device layer that is still anchored to the handle layer by the BOX layer which has not been released. In the center of the area is the patterned PnC. The upper right image is of a sample area which has had the same process performed on it as in the leftmost image. The Cr layer is still present in this image; its purpose is to protect the Si membrane from Ga ion implantation. Note that under the freestanding membrane are holes in the handle layer which correspond to the holes milled through the device layer. These holes serve as proof to full penetration of the device layer by the FIB. These thru holes are then backfilled with tungsten using a gas injection system (GIS) which introduces a precursor gas with W attached. When the precursor gas is exposed to an ion or electron beam W is deposited. An electron beam is directed in the center of the PnC inclusion holes and W is deposited to create a solid plug. Solid inclusion have been shown to create wider bandgaps in PnCs[3,4]. A cross section of the sample is shown in the lower right most image of Figure 2.

Phononics 2011: First International Conference on Phononic Crystals, Metamaterials and Optomechanics
Santa Fe, New Mexico, USA, May 29-June 2, 2011
PHONONICS-2011-0125

The operating frequency of 33 GHz was determined by simulation. Our group has developed several numerical tools for investigations of the behavior of PnCs[2,3,4]. These tools include the plane wave expansion (PWE) method, finite difference time domain (FDTD) method, and finite element analysis (FEA). Each method has its benefits and limitations. The PWE method allows us to determine bandgaps and density of states. While the FDTD and FEA methods allow us to determine bandgaps and vibrational modes. We find that using a commercial FEA software allows us to more accurately determine the behavior of devices under test by simulating the experimental conditions as well. Results from these simulations will be presented to supplement the new fabrication method introduced above and in the presentation.

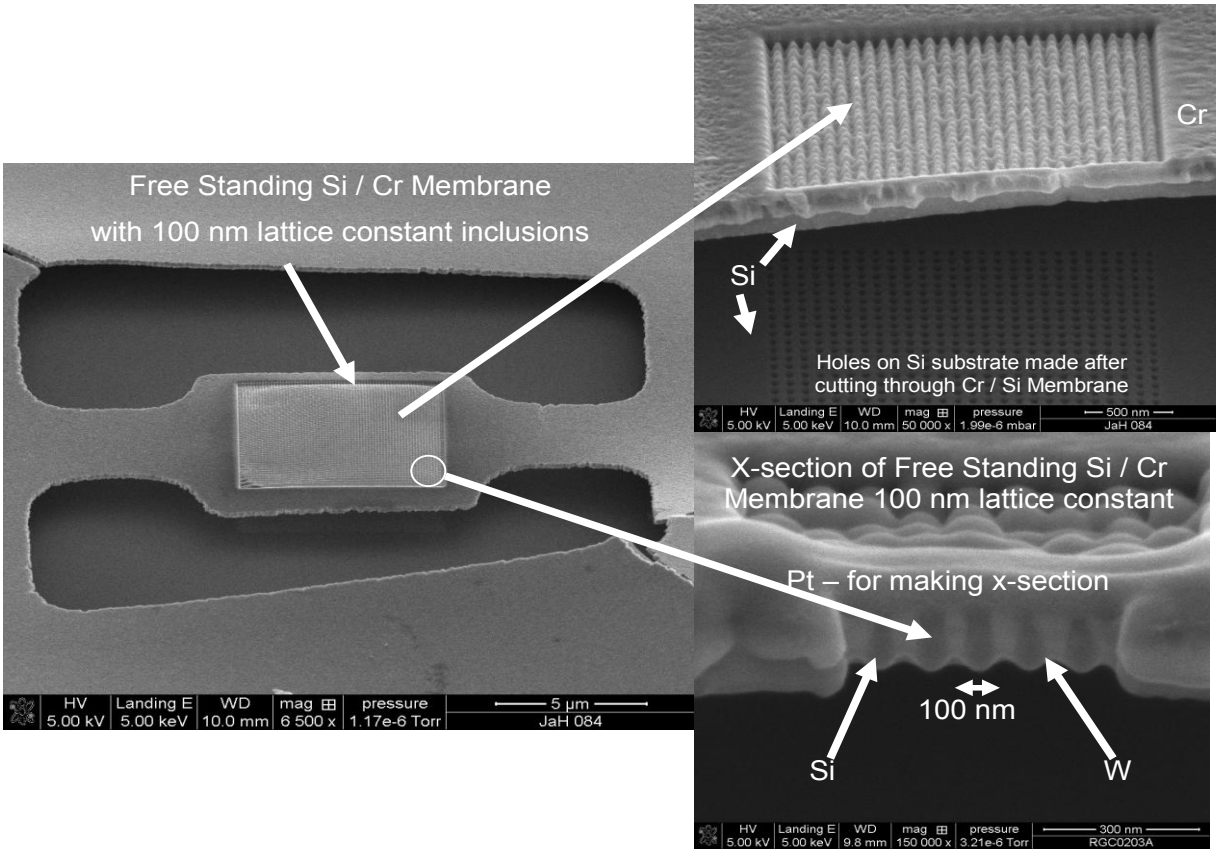

Figure 2: 33 GHz PnC fabricated with a focused ion beam with a 100 nm lattice constant and 30 nm W inclusions.

REFERENCES

[1]P. E. Hopkins, C. M. Reinke, M. F. Su, R. H. Olsson III, E. A. Shaner, Z. C. Leseman, J. R. Serrano, L. M. Phinney, and I. El-Kady, *Nano Letters*, **11**, (2011).

[2]M. F. Su, R. H. Olsson, Z. C. Leseman and I. El-Kady, *Appl. Phys. Lett.* **96** (2010).

[3]Y. M. Soliman, M. F. Su, Z. C. Leseman, I. El-Kady, R. H. Olsson III, *Appl. Phys. Lett.* **97** (2010).

[4]Y. M. Soliman, M. F. Su, Z. C. Leseman, C. M. Reinke, I. El-Kady, R. H. Olsson III, *Appl. Phys. Lett.* **97** (2010).

Phononics 2011: First International Conference on Phononic Crystals, Metamaterials and Optomechanics
Santa Fe, New Mexico, USA, May 29-June 2, 2011
PHONONICS-2011-0131

High Frequency Soft Phononics

George Fytas,[1,2,3] **Tim Still,**[1] **Dirk Schneider,**[1] **Nikos Gomopoulos,**[1] **Uli Jonas** [4]

[1] *Max Planck Institute for Polymer Research, P.O.Box 3148, 55128 Mainz, Germany*
[2] *Department of Materials Science and Technology, University of Crete, Heraklion, Greece*
[3] *FORTH, Institute of Electronic Structure & Laser (IESL), P.O. Box 1527, 71110 Heraklion, Greece*
fytas@mpip-mainz.mpg.de
[4] *FORTH, Bio-Organic Materials Laboratory (BOMBCLab), P.O. Box 1527, 71110 Heraklion, Greece*

Abstract: Propagation of hypersonic elastic/acoustic waves in polymer- and colloid-based nanostructures emerges as a powerful characterization tool of thermo- mechanical properties and reveals new structure related collective phenomena .Particle vibration spectroscopy and engineering of the phonon dispersion band diagram are highlighted in this presentation.

Phononic crystals become the acoustic equivalents of the photonic crystals controlled, however, by a larger number of material parameters. In contrast to the sonic and ultrasonic crystals, the study of hypersonic crystals (at the submicron scale), imposes substantial demand on fabrication and characterization techniques. Colloid and polymer science offer methods to create novel materials that possess periodic variations of density and elastic properties at mesoscopic length scales commensurate with the wave length of hypersonic phonons and hence photons of the visible light. Polymer-and colloid-based phononics is an emerging new field at the interface of soft materials science and condensed matter physics with rich perspectives ahead.

The key quantity for phononics is the dispersion of high frequency (GHz) acoustic excitations in mesoscopic structures which is nowadays at best measured by high resolution spontaneous Brillouin light scattering (BLS) at thermal equilibrium. Depending on the components of the nanostructured composite materials, the resolved vibration eigenmodes (the music) of the individual particles sensitively depend on the particle architecture and their thermo-mechanical properties. In periodic structures (the concert) of polymer based colloids, the dispersion relation $\omega(k)$ between the frequency and the phonon wave vector k has revealed hypersonic phononic band gaps of different nature.

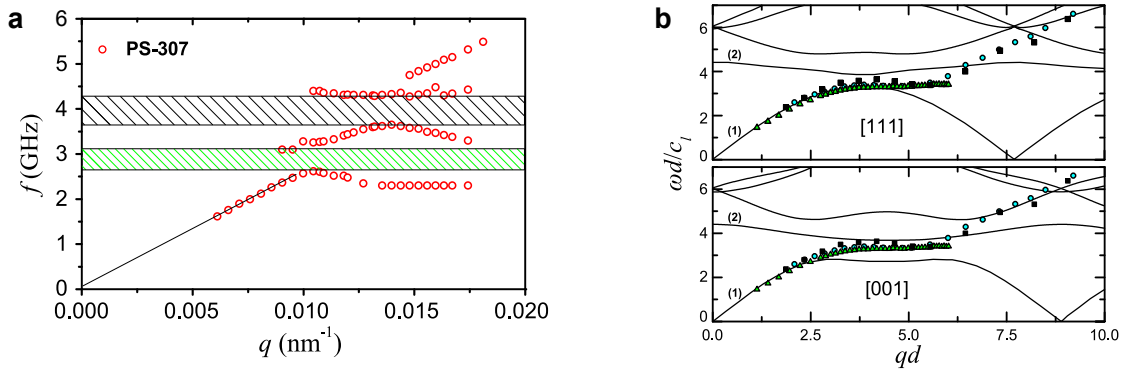

Figure 1 Phononic band diagram for an elastically soft polystyrene (PS) **(a)** and hard SiO_2 **(b)** colloidal crystal. Hybridization (green) and Bragg band gap (gray hatched area) in **(a)** and slow phonons (experimental points) due to strong coherent multiple scattering in a fcc crystal of closely packed SiO_2 spheres (three different diameters d=192nm (triangles) 354nm (circles) and 632nm (squares)) along its two symmetry directions in **(b)**.

Bragg gap for propagation near the edge of the first Brillouin zone due to destructive interference and hybridization gap due to the interaction of particle eigenmodes with the effective medium acoustic branch; the latter is therefore robust against structural. This seems to be the case for colloidal crystals based on elastically soft particles (Fig.1a). Boosting the strength of the phonon scattering by the individual spheres,

Phononics 2011: First International Conference on Phononic Crystals, Metamaterials and Optomechanics
Santa Fe, New Mexico, USA, May 29-June 2, 2011
PHONONICS-2011-0131

e.g., elastically hard SiO_2 particles can activate additional mechanisms for tunability of the phononic band structure as indicated in Fig.1b. In contrast to soft colloidal crystals, the phonon dispersion of dense SiO_2 colloids exhibits novel and unexpected features. Apart from the extended effective-medium band (1) and narrow bands stemming from localized particle resonances at relatively high frequencies, we identified additional almost dispersionless collective modes (2) at lower frequencies. These originate from strong coherent phonon multiple scattering and are localized in regions of the fluid matrix; their bending arises from strong hybridization. The elucidation of all important parameters towards the general design of optimal phononic structures remains complicated due to the vector nature of elastic wave propagation. In this regard, 1D phononic crystals (SiO_2/PMMA) multilayer films turn out to be a model system. Since hypersonic crystals can simultaneously exhibit phononic and photonic band gaps in the visible spectral region, many technological applications are feasible.

Like small molecules colloidal particles undergo vibrational motions, e.g., and shape fluctuations due to thermal energy. The acoustic vibrations of free homogeneous spheres predicted by Lamb in 1882, are classified as torsional and spheroidal ones and their frequencies $\omega(n,l)$, depend on the diameter and the elastic constants of the particle. For submicron sizes, BLS is the most sensitive technique to probe numerous eigenmodes in GHz frequencies and reveal the $\omega(n,l) \sim d^{-1}$ scaling for the spheroidal modes with order n and angular momentum "quantum number" l. The estimation of the thermo-mechanical properties (T_g, Young's and shear moduli) at nanoscale, which can deviate from the bulk values, is straightforward, provided a unique assignment of all observed eigenmodes is warranted. This requires a consensus on the existence of "selection rules" and on the contribution of torsional modes in the BLS spectra. These two important issues have very recently addressed through the full theoretical account of the experimental spectrum $I(\omega(n,l),q)$ at different probing wave vectors q. It is the dependence on qd that selects which spheroidal modes will be revealed experimentally. This emerging particle vibration spectroscopy for spherical shape has rich perspectives. Different particle morphologies, extension to non-spherical particles and the possibility to sense particle interactions are now being unexplored. Understanding of elastic energy localization in different compartments of the nanostructures is a precondition to access fundamental concepts such as engineering the flow of elastic energy and nanomechanics.

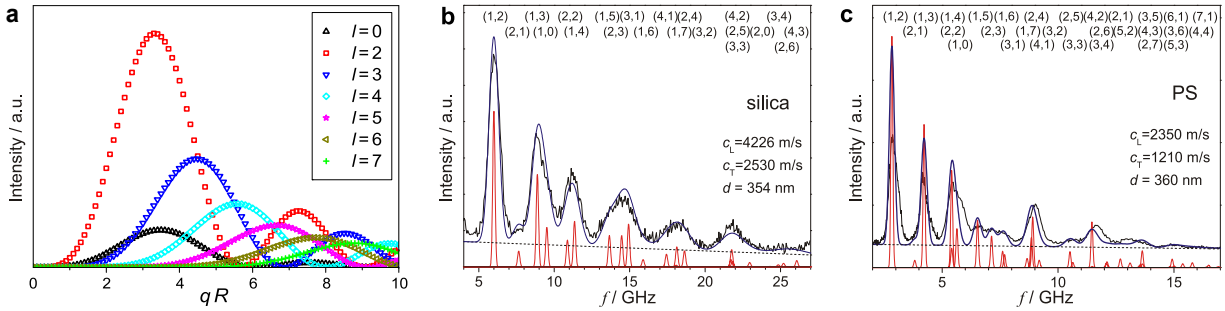

Figure 1 (a) The amplitude of the fundamental ($n = 1$) vibrational eigenmodes with $l = 0$ and $2 \le l \le 7$ for a free vibrating polystyrene (PS) latex spheres as a function of the product of the scattering wave vector q and particle radius R. **(b, c)** Comparison between experimental (black solid line) and calculated (blue) eigenmode spectra of SiO2 and PS spheres (diameter d). The sharp red lines denote the contribution of the individual $(n.l)$ modes labeled in the plots and the blue line is the sum of all modes.

References

[1] W. Cheng, M. Retsch, U. Jonas, G. Fytas, N. Stefanou, *Nature Mater.* **5**, 830 (2006).
[2] T. Still, W. Cheng, M. Retsch, R. Sainidou, J. Wang, U. Jonas, N. Stefanou, G. Fytas, *Phys. Rev. Lett.* **100**, 194301 (2008).
[3] N. Gomopoulos, D. Maschke, C. Y. Koh, E. L. Thomas, W. Tremel, H.-J. Butt, G. Fytas, Nano Lett. 10, 980 (2010).
[4] W. Cheng, J. Wang, U. Jonas. W. Steffen, G. Fytas, R. S. Penciu, E. N. Economou, J. Chem. Phys. 123, 121104 (2005).
[5] T. Still, R. Sainidou, M. Retsch, U. Jonas, P. Spahn, G. Hellmann, G. Fytas, Nano Lett. 10, 3194 (2008).
[6] T. Still, M. Mattarelli, D. Kiefer, G. Fytas, M. Montagna, *J. Phys. Chem. Lett.* **1**, 2440 (2008).

Phononics 2011: First International Conference on Phononic Crystals, Metamaterials and Optomechanics
Santa Fe, New Mexico, USA, May 29-June 2, 2011
PHONONICS-2011-0143

Techniques for Self-Assembled Phononic Crystals

T. J. Isotalo[1] , N. Zen[1], Y. Tian[1], I. J. Maasilta[1]

[1] *Nanoscience Center, Department of Physics, University of Jyväskylä, P.O. Box 35 FIN 40014, Finland,*
tero.isotalo@phys.jyu.fi, ilari.maasilta@phys.jyu.fi

Abstract: In this project, we study the assembly of periodic arrays of nanospheres and their crystalline properties. The vertical deposition technique is investigated along with the effects of substrate surface modifications for improvement of order and directed self-assembly. Dipping speed and PS sphere concentration are taken as the primary parameters affecting crystalline quality.

Arrays of monodisperse spherical particles, known as artificial opals, are commonly used to make photonic crystals for various applications. Similarly, an ordered array of spherical particles should exhibit a phononic band gap depending on the particle diameter. At temperatures around 100 mK, the thermal phonon wavelength is on the order of 100 nm. Thus, the thermal properties of phononic crystals made from 260 nm and 140 nm spheres should be strongly modified, and will be studied at sub-Kelvin temperatures using tunnel junction thermometry.

A vertical deposition technique [1], spinning and simple gravitational deposition [2] have been examined as methods for the fabrication of self-assembled arrays of nanospheres. Solutions of 10% and 2% of polystyrene (PS) nanospheres were studied on substrates of silicon, thermally grown SiO_X, PECVD SiN_X and glass, using a thin layer of Ti to provide an adhesion layer [3]. Hexagonal close packed structures have been produced with some regions exhibiting a cubic lattice. Directed self-assembly [4,5] of PS sphere arrays, 1-D chains and individual sphere placement was also investigated by using the vertical deposition method on substrates with patterned surfaces. Additionally, direct e-beam lithography of poly-methyl methacrylate (PMMA) nanospheres has been tested. Verifying the resulting lattice structures of deposited nanospheres was performed with scanning electron microscopy (SEM).

Experimental Methods

Of the three deposition methods investigated, the vertical deposition process appears to have the greatest utility and potential for reproducible monolayer and multi-layer arrays of polystyrene spheres. Spinning resulted in significantly lower order even at speeds of ~500 rpm. Gravitational deposition involved placing a droplet on the substrate surface and allowing the spheres to sediment during drying. Though noticeably greater order was observed, this method is inherently inconsistent from one sample to another as well as across individual sample surfaces. While the dipping process is time consuming, it is simple and reliable. A thin film of UHV evaporated Ti can be used to significantly improve adhesion on glass and SiN_X substrates. The samples are dipped either vertically or at an angle of 45° into the solution and withdrawn again. The angled depositions tend to give a lower quality film compared to vertical. This is likely due to dynamics of the contact angle between solution meniscus and substrate [6]. To further probe the control of crystalline quality, dipping speed and PS sphere concentration were studied as controls for domain size. Dipping speeds of 0.01 mm/min up to 0.1 mm/min were investigated with concentrations of 10, 2, 0.2 and 0.02%. Images were taken at several locations on each sample using SEM. Figure 1 shows an example of a measurement image. A rough estimate of domain area was obtained by taking length and width measurements of the domains and multiplying the two values. Measurement data from all the images were collected and used

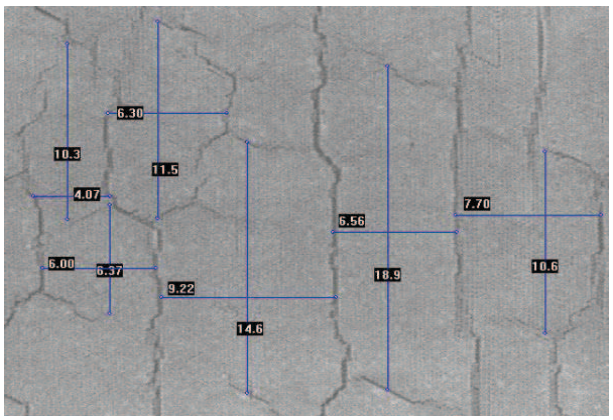

Figure 1 SEM image shows an example of domain measurements. An approximate area for domains is obtained by multiplying these length and width values.

Phononics 2011: First International Conference on Phononic Crystals, Metamaterials and Optomechanics
Santa Fe, New Mexico, USA, May 29-June 2, 2011
PHONONICS-2011-0143

to get an average value for the whole sample. From these images, one can also find indications of directionality in the domains. This effect tends to follow the dipping direction, with higher speeds displaying greater directionality.

Results

As expected, lower dipping speed results in larger domains. With slower speeds, the spheres have a longer time in contact with the substrate while in solution, allowing development of long-range order. However, there appears to be an optimum dipping speed at a given concentration, above and below which the quality declines. At higher than optimum speeds for a given concentration, there is little if any aggregation. The result is that spheres are located in small groups of three or four across most of the sample surface. Below the optimum speed, domain size varies greatly and thus results are unreliable. While a few larger domains are found, the variation is larger than the change in average domain size from one dipping speed to the next. Concentration follows a similar pattern. Higher concentrations produce larger domains and lower concentrations produce smaller domains. There is of course, a limit below which aggregation is no longer present. With lower concentrations at the same dipping speed, the size dispersion of domains is smaller indicating that consistency in long-range order suffers with increasing concentration.

An estimate of the number of layers deposited was also obtained using a profilometer. While the precise number of layers is not reliably measured in this way, a relation between dipping speed, PS sphere concentration and thickness can be discerned. Again, as expected, lower dipping speed and higher concentration result in greater thickness. The nanosphere arrays in this study ranged in thickness from 1 to approximately 20 layers. Gathering information about ordering in the thickness direction has been difficult for lack of a reliable method to image the side face without significantly changing the self-assembly conditions or altering the structure in post-processing.

Conclusions and prospects

The fabrication of thick and large area self-assembled phononic crystals requires time. The results of this study show that simply slowing down the process, however, is not sufficient to increase the domain size. PS sphere concentration plays a significant role in domain size and needs to be considered in parallel with dipping speed. We have shown initial trends for these two parameters and further development is ongoing.

Initial tests of directed self-assembly of nanosphere arrays are promising. Standard e-beam lithography techniques are used to produce channels of different shapes and sizes into which the nanospheres are selectively deposited. Arrays with dimensions in tens of microns are reproducible while chains and individual placement have shown positive results. Lithographically directed self-assembly can be used to place individual spheres on the substrate surface, allowing even more freedom to design the array patterns. Lithographic methods may also allow for imaging of the side wall to observe ordering in the thickness direction.

Direct lithography of PMMA nanospheres also shows promise. Different geometries have been patterned into pre-assembled PMMA sphere arrays. Reproducible lithography will still require some development in the alignment process. Ongoing experiments are focused on improving pattern design and further increasing the size of ordered domains.

References

[1] Z. Lü, W. Ruan, N. Ji, L. Ren, Q. Cong, B. Zhao, *J. Bionic Eng.* **3**, 059 (2006).
[2] Y. Xia, B. Gates, Y. Yin, Y. Lu, *Adv. Mater.*, **12**, 693 (2000).
[3] S. Karuppuchamy, J.M. Jeong, *Mater. Chem. Phys* **93**, 251 (2005).
[4] M. Allard, E.H. Sargent, P.C. Lewis, E. Kumacheva, *Adv. Mater.* **16**, 1360 (2004).
[5] C.A. Fustin, G. Glasser, H.W. Spiess, U. Jonas, *Langmuir* **20**, 9114 (2004).
[6] P.I. Stavroulakis, N. Christou, D. Bagnall, *Mater. Sci. Eng. B* **165**, 186 (2009).

Phononics 2011: First International Conference on Phononic Crystals, Metamaterials and Optomechanics
Santa Fe, New Mexico, USA, May 29-June 2, 2011
PHONONICS-2011-0151

The Effect of Phononic Crystal Lattice Type and Lattice Spacing on the Reduction of Bulk Thermal Conductivity in Silicon and Silicon Nitride

Drew F. Goettler[1], Bongsang Kim[2], Roy H. Olsson III[2], Zayd C. Leseman[1], Charles M. Reinke[2], Ihab I. El-Kady[2]

[1] *Mechanical Engineering, University of New Mexico, Albuquerque, NM, USA,*
goettled@unm.edu, zleseman@unm.edu
[2]*Sandia National Laboratories, Albuquerque, NM, USA*
bonkim@sandia.gov, rholsso@sandia.gov, cmreink@sandia.gov, ielkady@sandia.gov

Abstract: Phononic crystals are a promising method of reducing a material's bulk thermal conductivity. Changing a phononic crystal's lattice type or its lattice spacing are two ways of reducing a material's thermal conductivity. Results of different lattice types and lattice spacings on the reduction of bulk thermal conductivity in silicon and silicon nitride at room temperature will be presented.

Phononic crystals (PnCs) were recently shown to reduce the thermal conductivity of bulk silicon by more than an order of magnitude[1]. The PnCs were fabricated using photolithography and utilized a two-dimensional simple cubic pattern with a lattice constant ranging between 800 and 500 nm.

As an alternative to using photolithography for fabricating phononic crystal arrays, a focused ion beam (FIB) can fabricate various patterns in a short amount of time without the need for additional photolithography masks. In this report, we use two different setups to measure the thermal conductivity of PnCs fabricated in silicon and silicon nitride with a FIB. The first setup uses a heater in the middle of two identical PnCs on a freestanding Si membrane 500 nm thick. Current flowing through the resistive element provides joule heating. Due to symmetry, half of the heat flows to each side of heater. Temperature sensors, which are calibrated prior to the experiments, are located at each end of the phononic crystal and measure the temperature of the Si. By knowing the amount of heat flowing into the system, the change in temperature across the phononic crystal, and the PnC's dimensions, a thermal conductivity of the specimen can be calculated using

$$k_{PnC} = \frac{Q_{heat}}{2wt\Delta T} \tag{1}$$

where k_{PnC} is the effective thermal conductivity of the PnC, Q_{heat} is the input heat, w and t are the width and thickness of the PnC, and ΔT is the change in temperature across the PnC.

The second set up, based on a design by Li Shi[2], is used to measure the thermal conductivity of a PnC in silicon nitride. In this configuration, a thin strip of silicon nitride containing a PnC milled with the FIB separates two freestanding islands of silicon nitride. Since the islands and the PnC are made of the same material, there is no worry of contact resistance. Each island is supported by four legs 1 μm wide. One island acts as a heat source, and the other island is the sensing island. A top view of this set up is shown in Figure 1.

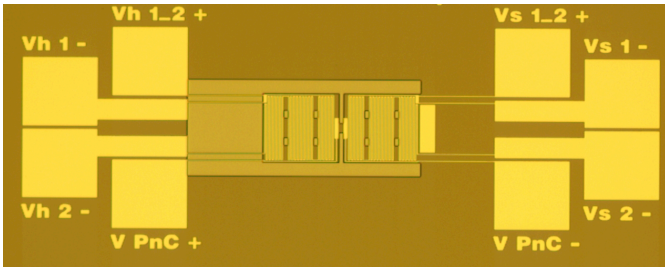

Figure 1 Set up for determining thermal conductivity of silicon nitride PnC. The two islands are separated by a 5x15 μm area of silicon nitride.

Phononics 2011: First International Conference on Phononic Crystals, Metamaterials and Optomechanics
Santa Fe, New Mexico, USA, May 29-June 2, 2011
PHONONICS-2011-0151

In the middle of the figure are the two suspended islands with platinum serpentine heaters on top of each silicon nitride membrane island. Each heater is connected to contact pads by metal lines on the support legs. Between the islands is a small area of silicon nitride where the PnC is fabricated. Isolation of the two islands forces a majority of the heat to flow across the silicon nitride PnC. Finite element analysis performed with ANSYS shows a uniform temperature distribution on the heating island and on the sensing island as well (see Figure 2). This supports the assumption that the silicon nitride PnC can be treated as a one-dimensional component.

Results from both setups will be presented.

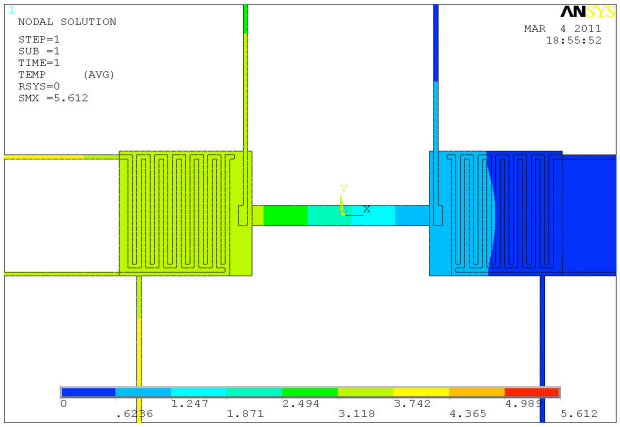

Figure 2 FEM analysis of temperature gradient across silicon nitride membrane connecting heating and sensing island. A temperature scale bar is shown at the bottom, where red indicates a higher temperature and blue corresponds to a lower temperature. Notice the uniform temperature of the heating island (yellow) and planar heat flow across the sensing island (blue). ANSYS was used to perform the FEM analysis.

References

[1] P. E Hopkins, C. M. Reinke, M. F. Su, R. H. Olsson III, E.A. Shaner, Z. C Leseman, J. R. Serrano, L. M. Phinney, I. El-Kady, *Nano Lett*, **11**, 107-112, (2011).
[2] L. Shi, Ph.D thesis, University of California, Berkley, (2001).

Phononics 2011: First International Conference on Phononic Crystals, Metamaterials and Optomechanics
Santa Fe, New Mexico, USA, May 29-June 2, 2011
PHONONICS-2011-0158

Nanophononics using Acoustic and Optical Cavities

N. D. Lanzillotti-Kimura[1,2], A. Fainstein[1], B. Jusserand[3], B. Perrin[3], A. Lemaitre[4], D. G. Schlom[5], A. Soukiassian[5]

[1] *Centro Atómico Bariloche & Instituto Balseiro, C.N.E.A., R8402 AGP S. C. De Bariloche, Río Negro, Argentina*
kimura@cab.cnea.gov.ar, afains@cab.cnea.gov.ar
[2] *University of California – Berkeley, CA 94720, USA*
[3] *Institut des NanoSciences de Paris, CNRS – Université Pierre et Marie Curie, 75004 Paris, France*
bernard.jusserand@insp.jussieu.fr, bernard.perrin@insp.jussieu.fr
[4] *Laboratoire de Photonique et des Nanostructures, C.N.R.S., Route de Nozay, 91460 Marcoussis, France aristide.lemaitre@lpn.cnrs.fr*
[5] *Department of Materials Science and Engineering, Cornell University, Ithaca, New York, 14853-1501, USA*
ds636@cornell.edu, soukiassian@gmail.com

Abstract: We report pump-probe time experiments in acoustic and optical cavities. We demonstrate that the generated coherent acoustic phonon spectra can be inhibited or enhanced in the cavity. Simulations highlight the role of the phonon density of states in the coherent phonon generation, extending concepts at the base of the Purcell effect to the field of phononics.

Changing the spontaneous light emission rate and spectra of atoms or excitons through the modification of the photon density of states has been the subject of significant efforts following Purcell's proposal and demonstration in the microwave domain.[1] This has been accomplished either by changing the dielectric boundaries close to the emitting species, or more fundamentally by embedding the emitter in an optical microcavity.[2] Depending on the tuning of the emitter spectra with maxima or minima of the modified photonic density of states, the emission can be either enhanced or inhibited. Similar ideas have been applied to modify other light-matter interactions processes. The search for large Purcell effects is at the heart of the quest for thresholdless lasing. In the field of phononics, and specifically the search of phonon lasing for efficient monochromatic THz sources, and for the control of heat at the nanoscale, these ideas have not been pursued to date. Here we demonstrate that the coherent acoustic phonon emission spectra of an impulsively excited thin metallic film can be either inhibited or enhanced by embedding the metal layer in an acoustic nanocavity.[3-6] This has been accomplished by using for the first time a hybrid metal cavity with $BaTiO_3/SrTiO_3$ epitaxial oxide phonon mirrors.

Acoustic nanocavities are the hypersound analog of the extensively studied optical microcavities.[3-6] We use a femtosecond laser light impulsion to generate a pulse of coherent sub-THz phonons in a metallic layer, and then we study how the latter is modified by changing the structure around the metal film. We compared two samples, in the first one we deposited the Ni film directly on a $SrTiO_3$ substrate, while in the second one the film is embedded in an acoustic nanocavity. In the latter, we chose as bottom broadband acoustic mirror $BaTiO_3/SrTiO_3$ superlattice (SL) grown by molecular beam epitaxy on a $SrTiO_3$ substrate. $BaTiO_3$ and $SrTiO_3$ have optical energy gaps in the 350 nm range and are consequently completely transparent at the laser energy of 750 nm. In this way, the acoustic mirrors only affect the acoustic boundary conditions of the metallic film, and thus its local acoustic density of states. The sample-air interface responds to a free surface boundary condition. This surface performs as the top mirror to complete the phonon cavity. Both the coherent phonon generation and detection are performed only at the metallic films. In the case of the acoustic nanocavity the measured spectrum presents an enhanced peak at the confined mode energy, while in the case of the naked Ni film the spectrum is broad and featureless. Moreover, we observed the inhibition of the coherent phonon emission in the region of the acoustic stop-band. In other words, within the phononic stop-band modes are expelled and they concentrate at the cavity resonance and at the stop-band edges. It is this modification of the mode density landscape that determines at which energies acoustic phonons can be emitted by the metallic layer (enhancement at the cavity mode), and at which they cannot (inhibition within the phonon gap). In addition, outside the phononic stop-band oscillations develop in the generated spectrum which, when compared with the bare Ni-film, also express weaker but clear inhibition and enhancement regions. The experiments are compared with calculations of the impulsive

Phononics 2011: First International Conference on Phononic Crystals, Metamaterials and Optomechanics
Santa Fe, New Mexico, USA, May 29-June 2, 2011
PHONONICS-2011-0158

generation and detection of coherent phonons that highlight the role of the phonon density of states on the acoustic emission rate, extending the concept of the optical Purcell effect to the field of phononics.

In addition, we report experiments performed on structures based in semiconductor optical microcavities, where acoustic phonons and photons can be confined simultaneously. Thus, both the optical and acoustic densities of states result modified.[7-8] An optical microcavity confines the electromagnetic field both spectrally and spatially, inducing strong changes in the light-matter interaction and giving rise to novel physical phenomena and devices. In the case of planar semiconductor optical microcavities, two distributed Bragg reflectors (DBRs) enclose an optical spacer. The confinement characteristics and the amplification of the electric field are determined by the selection of materials, thickness, and number of periods that constitute each DBR and the optical spacer. Optical microcavities have been the subject of very active research during the last 15 years, and have been used to study the modification of the photonic lifetimes, parametric oscillations, cavity polariton Bose-Einstein condensates, the polariton laser, and amplification of Raman scattering signals, among others.[9-11]

Particularly, the photonic confinement and amplification have been used in these high-Q resonators to amplify the optical generation of incoherent phonons through Raman processes and to evidence new effects in the phonon physics and dynamics in semiconductor nanostructures. This scheme was used to study confined phonons in acoustic nanocavities. The optical resonances can be complemented with electronic resonances giving rise to amplified Raman cross-sections of up to 10^7. On the contrary, the use of optical confinement for the enhanced coherent generation of acoustic phonons (in contrast with incoherent generation by spontaneous Raman scattering) is a concept that has been little treated up to now. The realization of a monochromatic, coherent, and intense source of ultrahigh frequency acoustic phonons based on semiconductor optical microcavities and the obtained coherent phonon enhancements will be also discussed.

References

[1] E. Purcell, in Proceedings of the American Physical Society, 1946 [Phys. Rev. **69**, 681 (1946)].
[2] E. Yablonovitch, Phys. Rev. Lett. **58**, 2059 (1987).
[3] M. Trigo, A. Fainstein, B. Jusserand, and V. Thierry-Mieg, *Phys. Rev. Lett.* **89**, 227402 (2002).
[4] A. Huynh, N. D. Lanzillotti-Kimura, B. Jusserand, B. Perrin, A. Fainstein, M. F. Pascual-Winter, E. Peronne, and A. Lemaître, Phys. Rev. Lett. **97**, 115502 (2006)
[5] N. D. Lanzillotti-Kimura, A. Fainstein, A. Huynh, B. Perrin, B. Jusserand, A. Miard, and A. Lemaître, *Phys. Rev. Lett.* **99**, 217405 (2007).
[6] A. Huynh, B. Perrin, N. D. Lanzillotti-Kimura, B. Jusserand, A. Fainstein, and A. Lemaître, Phys. Rev. B **78**, 233302 (2008)
[7] N. D. Lanzillotti-Kimura, A. Fainstein, B. Jusserand, and A. Lemaître, Phys. Rev. B **79**, 035404 (2009)
[8] N. D. Lanzillotti-Kimura, A. Fainstein, B. Perrin, B. Jusserand, A. Soukiassian, X. X. Xi, and D. G. Schlom, *Phys. Rev. Lett.* **104**, 187402 (2010).
[9] D. Sanvitto, F. M. Marchetti, M. H. Szymanska, G. Tosi, M. Baudisch, F. P. Laussy, D. N. Krizhanovskii, M. S. Skolnick, L. Marrucci, A. Lemaître, J. Bloch, C. Tejedor, and L. Vina, Nature Physics **6**, 527 (2010)
[10] E. Wertz, L. Ferrier, D. D. Solnyshkov, R. Johne, D. Sanvitto, A. Lemaître, I. Sagnes, R. Grousson, A. V. Kavokin, P. Senellart, G. Malpuech and J. Bloch, Nature Physics **6**, 860 (2010)
[11] A. Fainstein and B. Jusserand, Light scattering in Solids IX: Novel Materials and Techniques 108, 17, (Springer, Heidelberg, (2007)

Phononics 2011: First International Conference on Phononic Crystals, Metamaterials and Optomechanics

Santa Fe, New Mexico, USA, May 29-June 2, 2011

PHONONICS-2011-0164

nanoFIBrication of Phononic Crystals in Freestanding Membranes

D. F. Goettler[1], M. F. Su[1], R. H. Olsson III[2], I. El-Kady[2], and Z. C. Leseman[1*]

[1] Mechanical Engineering, University of New Mexico, Albuquerque, NM USA 87131
goettled@unm.edu, mfatihsu@unm.edu, and zleseman@unm.edu
[2] Sandia National Laboratories, Albuquerque, NM USA 87105
rholsso@sandia.gov and ielkady@sandia.gov

Abstract: For this poster, we describe a novel method for the fabrication of phononic crystals in freestanding membranes using a method dubbed 'nanoFIBrication.' The method is demonstrated by nanoFIBricating a 35 GHz phononic crystal. Post fabrication of phononic crystals shows that the vias flare out at their exit, which we call the 'trumpet effect.'

For this poster, we describe a novel method for the fabrication of phononic crystals in freestanding membranes using a method dubbed 'nanoFIBrication.' The method is demonstrated by nanoFIBricating a 35 GHz phononic crystal. Initially, a square array of vias with 150 nm spacing (center-to-center) is generated over an area of 6.75 x 6.75 μm. The vias are then backfilled with void-free tungsten. Each tungsten plug has a diameter of 48 nm – these constitute the scatterers of the phononic crystal. A protective layer of chromium is used to minimize the amount of contamination by Ga from the focused ion beam. The chromium is removed at the end of the process. Post fabrication of phononic crystals shows that the vias flare out at their exit, which we call the 'trumpet effect.' The trumpet effect is explained by modeling the lateral damage in the freestanding member via Monte Carlo simulations.

Phononics 2011: First International Conference on Phononic Crystals, Metamaterials and Optomechanics

Santa Fe, New Mexico, USA, May 29-June 2, 2011

PHONONICS-2011-0164